INTERNATIONAL JOURNAL OF ROBUST AND NONLINEAR CONTROL
Int. J. Robust. Nonlinear Control 2017; **00**:1–18
Published online in Wiley InterScience (www.interscience.wiley.com). DOI: 10.1002/rnc

Quantization effects and convergence properties of rigid formation control systems with quantized measurements

Zhiyong Sun[1,*], Héctor Garcia de Marina[2], Brian D. O. Anderson[13], Ming Cao[4]

[1] *Data61-CSIRO (formerly NICTA) and Research School of Engineering, The Australian National University, Canberra ACT 2601, Australia.*
[2] *Ecole Nationale de l'Aviation Civile (ENAC), Toulouse, France.*
[3] *School of Automation, Hangzhou Dianzi University, Hangzhou 310018, China.*
[4] *Faculty of Mathematics and Natural Sciences, ENTEG, University of Groningen, The Netherlands.*

SUMMARY

In this paper we discuss quantization effects in rigid formation control systems when target formations are described by inter-agent distances. Because of practical sensing and measurement constraints, we consider in this paper distance measurements in their quantized forms. We show that under gradient-based formation control, in the case of uniform quantization, the distance errors converge locally to a bounded set whose size depends on the quantization error, while in the case of logarithmic quantization, all distance errors converge locally to zero. A special quantizer involving the signum function is then considered with which all agents can only measure coarse distances in terms of binary information. In this case the formation converges locally to a target formation within a finite time. Lastly, we discuss the effect of asymmetric uniform quantization on rigid formation control. Copyright © 2017 John Wiley & Sons, Ltd.

Received . . .

KEY WORDS: Rigid formation control; Quantization effect; Binary measurement.

1. INTRODUCTION

Quantized control has been an active research topic in the recent decade, motivated by the fact that digital sensors and numerous industrial controllers can only generate quantized measurements or feedback signals [1,2]. Recent years have also witnessed extensive discussions on quantized control for networked control systems. This is because data exchange and transmission over networks often occurs in a digitally quantized manner, thus giving rise to coarse and imperfect information; see e.g., [3–8].

In this paper, we aim to discuss the quantization effect on rigid formation control. Formation control based on graph rigidity is a typical networked control problem involving inter-agent measurements and cooperations. There have been many papers in the literature focusing on control performance and convergence analysis for rigid formation control systems (see e.g. [9–14]), with virtually all assuming that all agents can acquire the relative position measurements to their neighbors perfectly. We remark that there are some recent works on linear-consensus-based formation control with quantized measurements. An exemplary paper along this line of research is [15], which showed that by using very coarse measurements (i.e., measurements in terms of binary information) the formation stabilization task can still be achieved. The case of coarse measurements

*Correspondence to: Zhiyong Sun, zhiyong.sun@anu.edu.au, Research School of Engineering, The Australian National University, Canberra, ACT 2601, Australia.

can be seen as a special (or extreme) quantizer, which generates quantized feedbacks in the form of binary signals. However, in [15] and similar works on linear-consensus-based formation control, a common knowledge of the global coordinate frame orientation is required for all the agents to implement the control law. This is a strict assumption and is not always desirable in practical formation control systems. Actually, it has been shown in [16] that coordinate orientation mismatch may also cause undesired formation motions in linear-consensus-based formation systems. All these restrictions and disadvantages are known to be avoidable in rigid formation control systems, in which any common knowledge of the global coordinate system is not required.

In the framework of quantized formation control, we also consider in the latter part of this paper a special quantizer described by the *signum* function. This part is motivated by the previous work [17] which discussed *triangular* formation control with coarse distance measurements involving the signum function. In this paper we will consider a more general setting, which extends the discussions from the triangular case in [17] to more general rigid formations.

The aim of this paper is to explore whether the introduction of quantized measurement and feedback can still guarantee the success of formation control, and to what extent the controller performance limits exist. Our broad conclusion is that quantization is not fatal, but may reduce performance in achieving a target formation.

In this paper, we focus on local convergence of target formations with general shapes, by assuming that initial formations are minimally and infinitesimally rigid, and are close to a target formation, which is a common assumption that has been widely used in many papers on rigid formation control; see e.g. [9, 12, 14, 18, 19]. We note that local stability is also a practical problem, arising when wind disturbs a formation away from its desired shape, and the original shape has to be recovered. Local convergence of formation shape also has practical significance. For example, agents can firstly assemble an approximate formation close to the desired shape, and then apply the control law to achieve the target formation guaranteed by the local convergence. Global analysis of formation convergence and stability is however only available for some particular and simple formation shapes (see e.g., [10] for 2-D triangular shape, [20] for 3-D tetrahedral shape, and [21] for 2-D triangulated formations), while global analysis for rigid formation systems with general shapes is a challenging and open problem. Global analysis of formation convergence is therefore beyond the scope of this paper and will not be discussed here.

A preliminary version of this paper was presented in [22]. The extensions of this paper compared to [22] include detailed proofs for all the key results which were omitted in [22], examples on several quantizer functions, and a new section to discuss the formation convergence when using an asymmetric uniform quantizer. Furthermore, simulation results which support the theoretical analysis are provided in this extended paper.

The remaining parts are organized as follows. Section 2 briefly reviews some background on graph rigidity and two commonly-used quantizer functions. Section 3 discusses the convergence of the formation systems under two quantized formation controllers. In Section 4 we show a special quantized formation controller with binary distance information. Section 5 focuses on the case of an asymmetric uniform quantizer and its performance. Some illustrative examples are provided in Section 6. Section 7 concludes this paper.

2. BACKGROUND AND PRELIMINARIES

2.1. Notations

Most notations used in this paper are fairly standard, and here we introduce some special notations that will find use in later analysis. The the operator col$(\cdot)$ defines the stacked column vector. For a given matrix $A \in \mathbb{R}^{n\times m}$, define $\overline{A} := A \otimes I_d \in \mathbb{R}^{nd\times md}$, where the symbol $\otimes$ denotes the Kronecker product and I_d is the d-dimensional identity matrix with $d = \{2, 3\}$. We denote by $||x||$ the Euclidean norm of a vector x, by $\hat{x} := \frac{x}{||x||}$ the unit vector of $x \neq 0$, and by $\tilde{x} := \frac{1}{||x||}$ the

DOI: 10.1002/rnc

reciprocal of the norm of $x \neq 0$. For a stacked vector $x := \left[x_1^\top, x_2^\top, \ldots, x_k^\top\right]^\top$ with $x_i \in \mathbb{R}^l, i \in \{1, \ldots, k\}$, we define the block diagonal matrix $D_x := \text{diag}\{x_i\}_{i\in\{1,\ldots,k\}} \in \mathbb{R}^{kl\times k}$.

2.2. Graph rigidity

Consider an undirected graph with m edges and n vertices, denoted by $\mathcal{G} = (\mathcal{V}, \mathcal{E})$ with vertex set $\mathcal{V} = \{1, 2, \cdots, n\}$ and edge set $\mathcal{E} \subseteq \mathcal{V} \times \mathcal{V}$. The neighbor set $\mathcal{N}_i$ of node i is defined as $\mathcal{N}_i := \{j \in \mathcal{V} : (i, j) \in \mathcal{E}\}$. We define an oriented incidence matrix $B \in \mathbb{R}^{n\times m}$ for the undirected graph $\mathcal{G}$ by assigning an *arbitrary* orientation for each edge. Note that for a rigid formation modelled by an *undirected* graph considered in this paper, the orientation of each edge for writing the incidence matrix can be defined arbitrarily and the stability analysis in the next sections remains unchanged. By doing this, we define the entries of B as $b_{ik} = -1$, if $i = \mathcal{E}_k^{\text{tail}}$, or $b_{ik} = +1$, if $i = \mathcal{E}_k^{\text{head}}$, or $b_{ik} = 0$ otherwise, where $\mathcal{E}_k^{\text{tail}}$ and $\mathcal{E}_k^{\text{head}}$ denote the tail and head nodes, respectively, of the edge $\mathcal{E}_k$, i.e. $\mathcal{E}_k = (\mathcal{E}_k^{\text{tail}}, \mathcal{E}_k^{\text{head}})$. For a connected undirected graph, one has $\text{null}(B^\top) = \text{span}\{\mathbf{1}_n\}$.

We denote by $p = [p_1^\top, p_2^\top, \cdots, p_n^\top]^\top \in \mathbb{R}^{dn}$ the stacked vector of all the agents' positions $p_i \in \mathbb{R}^d$. We also define *non-collocated* positions for all agents as those positions for which $p_i \neq p_j$ for all $(i, j) \in \mathcal{E}$. The pair $(\mathcal{G}, p)$ is said to be a framework of $\mathcal{G}$ in $\mathbb{R}^d$. The incidence matrix B defines the sensing topology of the formation, i.e. it encodes the set of available relative positions that can be measured by the agents. One can construct the stacked vector of available relative positions by

$$z = \overline{B}^\top p, \tag{1}$$

where each element $z_k \in \mathbb{R}^d$ in z is the relative position vector for the vertex pair defined by the edge $\mathcal{E}_k$.

Let us now briefly recall the notions of infinitesimally rigid framework and minimally rigid framework from [23] and [24]. Define the edge function $f_{\mathcal{G}}(p) := \underset{k}{\text{col}}\left(\|z_k\|^2\right)$ where the operator col defines the stacked column vector. We denote the Jacobian of $\frac{1}{2}f_{\mathcal{G}}(p)$ by $R(z)$, which is called the *rigidity matrix*. An easy calculation shows that $R(z) = D_z^\top \overline{B}^\top$. A framework $(\mathcal{G}, p)$ is *infinitesimally rigid* if $\text{rank}(R(z)) = 2n - 3$ when it is embedded in $\mathbb{R}^2$ or if $\text{rank}(R(z)) = 3n - 6$ when it is embedded in $\mathbb{R}^3$. If additionally $|\mathcal{E}| = 2n - 3$ in the 2D case or $|\mathcal{E}| = 3n - 6$ in the 3D case then the framework is called *minimally rigid*. In this paper we assume that the target formation is infinitesimally and minimally rigid, while the convergence results obtained in this paper can be extended to non-minimally but still infinitesimally rigid target formations by following the analysis in [18] or [14].

2.3. Quantizer functions

In this paper, we mainly consider two types of quantizers: the uniform quantizer and the logarithmic quantizer [4–8]. In later sections we will also consider two special quantizers, namely a quantizer involving the signum function and the asymmetric uniform quantizer, derived from these quantizer functions.

2.3.1. Definition of the quantizers The *symmetric* uniform quantizer is a map $q_u : \mathbb{R} \to \mathbb{R}$ such that

$$q_u(x) = \delta_u \left(\left\lfloor \frac{x}{\delta_u} \right\rceil \right), \tag{2}$$

where δ_u is a positive number and $\lfloor a \rceil, a \in \mathbb{R}$ denotes the nearest integer to a. We also define $\lfloor \frac{1}{2} + h \rceil = h$ for any $h \in \mathbb{Z}$.

The *logarithmic* quantizer is an odd map $q_l : \mathbb{R} \to \mathbb{R}$ such that

$$q_l(x) = \begin{cases} \exp(q_u(\ln x)) & \text{when } x > 0; \\ 0 & \text{when } x = 0; \\ -\exp(q_u(\ln(-x))) & \text{when } x < 0. \end{cases} \tag{3}$$

where $\exp(\cdot)$ denotes the exponential function.

DOI: 10.1002/rnc

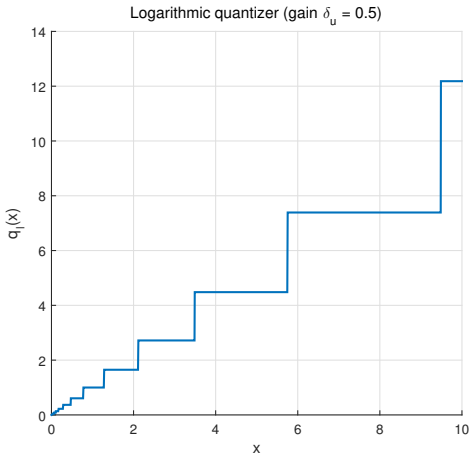

Figure 1. Logarithmic quantizer function with the gain $\delta_u = 0.5$, defined in (3).

2.3.2. Properties of the quantizers For the uniform quantizer, the quantization error is always bounded by $\delta_u/2$, namely $|q_u(x) - x| \leq \frac{\delta_u}{2}$ for all $x \in \mathbb{R}$.

For the logarithmic quantizer, it holds that $q_l(x)x \geq 0$, for all $x \in \mathbb{R}$, and the equality holds if and only if $x = 0$. The quantization error for the logarithmic quantizer is bounded by $|q_l(x) - x| \leq \delta_l|x|$, where the parameter δ_l is determined by $\delta_l = \exp(\frac{\delta_u}{2}) - 1$ (note that $\delta_l > 0$ because $\delta_u > 0$).

The above definitions for scalar-valued uniform and logarithmic quantizers can be generalized to vector-valued quantizers for a vector in a component-wise manner. For an illustration of a logarithmic quantizer function, see Figure 1. Note that in Section 5 we will further consider an *asymmetric* uniform quantizer, and will provide some comparisons between a *symmetric* uniform quantizer and an *asymmetric* uniform quantizer.

2.4. Nonsmooth analysis

Consider a differential equation

$$\dot{x}(t) = X(x(t)), \tag{4}$$

where $X : \mathbb{R}^d \to \mathbb{R}^d$ is a vector field which is measurable but discontinuous. The existence of a continuously differentiable solution to (4) cannot be guaranteed due to the discontinuity of $X(x(t))$. Also, as shown in [5], the Caratheodory solutions (for definitions, see [25]) may not exist from a set of initial conditions of measure zero in quantized control systems. Therefore, we understand the solutions to the quantized rigid formation system in the sense of Filippov [26]. We first introduce the Filippov set-valued map.

***Definition** 1*
Let $\mathcal{D}(\mathbb{R}^d)$ denote the collection of all subsets of $\mathbb{R}^d$. The Filippov set-valued map $F[X] : \mathbb{R}^d \to \mathcal{D}(\mathbb{R}^d)$ is defined by

$$\mathcal{F}[X](x) \triangleq \bigcap_{\delta>0} \bigcap_{\mu(\mathcal{S})=0} \overline{\text{co}}\{X(\mathbb{B}(x,\delta)\backslash\mathcal{S})\}, \quad x \in \mathbb{R}^d \tag{5}$$

where $\overline{\text{co}}$ denotes convex closure, $\mathcal{S}$ is the set of x at which $X(x)$ is discontinuous, $\mathbb{B}(x,\delta)$ is the open ball of radius δ centered at x, and $\bigcap_{\mu(\mathcal{S})=0}$ denotes the intersection over all sets $\mathcal{S}$ of Lebesgue measure zero.

Because of the way the Filippov set-valued map is defined, the value of $\mathcal{F}[X]$ at a discontinuous point x is independent of the value of the vector field X at x. Filippov solutions are absolutely continuous curves that satisfy almost everywhere the differential inclusion $\dot{x}(t) \in \mathcal{F}[X](x)$ defined

DOI: 10.1002/rnc

above. Some properties of the Filippov solution and examples of how to compute a Filippov set-valued map can be found in the review [25].

3. FORMATION CONTROL WITH QUANTIZED MEASUREMENTS

3.1. Quantized formation controllers

In rigid formation control each agent is required to measure the relative position (i.e. bearing and range) to its neighbors via a bearing sensor and a range sensor. If one assumes perfect measurements, a commonly-used formation controller can be written as (see e.g. [19, 27])

$$\dot{p}_i = -\sum_{k=1}^{m} b_{ik}(||z_k|| - d_k)\,\hat{z}_k, \tag{6}$$

where d_k is the desired distance for edge k which is adjacent with agent i , and other symbols appeared in (6) have been introduced in Sections 2.1 and 2.2. Note that more general forms of formation controllers to stabilize rigid formations are discussed in [14].

In the presence of quantized sensing and measurement, the right-hand side of the above formation control system (6) needs modification. Here we assume that the distance measurement (with an offset, see the following equation (7)) is quantized, and the bearing measurement is unquantized. This assumption is reasonable because the bearing measurement is always bounded (described by a unit vector, or by an angle in $[-\pi, \pi)$ in the 2-D case). A normal digital sensor, say a 10-bit uniform quantizer, applying to bearing measurements gives rather accurate measurement with very small error to the true bearing. This is not the case for distance measurements which may have larger magnitudes. We use quantized distance measurement in the formation controller design, while in the future work this may be relaxed by considering both quantized range and bearing measurements. With such considerations, a quantized formation control system can be written as

$$\dot{p}_i = -\sum_{k=1}^{m} b_{ik}\, q(||z_k|| - d_k)\,\hat{z}_k, \tag{7}$$

where q is a quantization function, which can be the uniform quantizer or the logarithmic quantizer defined in Section 2.3. We also assume that all the agents use the same quantizer $q(\cdot)$, and their initial positions start with non-collocated positions (which ensures $z_k(0) \neq 0$ for all k).

It is clear from (7) that each agent needs to measure relative position information (e.g., bearing and distance) to its neighbors. We also note that in practice agents could be equipped with sensors which produce separately the distance measurement and bearing measurement. For example, laser scanners or radars can give separately the range information (via round-trip travelling time of the signal) to its neighbors, and the bearing information to its neighbors in terms of $\hat{z}_k$ with respect to that agent's own local coordinate frame (as will be clarified later in Lemma 2).

Remark 1

One may wonder why there is not use of the quantization feedback in the form of $q(||z_k||)$, i.e. the direct quantized distance measurement, in the control (7). We note three reasons for choosing $q(||z_k|| - d_k)$ instead of $q(||z_k||)$, from the viewpoint of using quantization as a necessity (arising from limited measurement capabilities), and the advantages that are brought about by adopting such a quantization strategy:

- In rigid formation control, the control objective is to stabilize the actual distances between neighboring agents to prescribed values. If one chooses the quantization strategy in the form of $q(||z_k||)$, then this control objective may not be achieved. To this end, the quantization strategy $q(||z_k|| - d_k)$ used in (7) can be interpreted as arising from a digital distance sensor with an embedded or prescribed offset (where the offset is the desired distance d_k), which is practical in real-world applications.

DOI: 10.1002/rnc

- In the case of non-uniform quantizers (e.g., logarithmic quantizer), the quantization accuracy (or resolution) usually increases when the quantizer input approaches closer to the desired state (which is the origin in this case). Thus, when the formation approaches closer to the target formation, a higher quantization accuracy (if possible) is required, and this cannot be achieved if one uses the quantization function (e.g., logarithmic quantization) on the actual distance in the form of $q(||z_k||)$. Furthermore, such a quantization is appealing as a design choice as one can have finite time convergence (as proved in the later section), which is another advantage from the formation convergence viewpoint.
- We will further show in Section 4 that the chosen quantization strategy $q(||z_k|| - d_k)$ will specialize to a simple and effective quantizer with *coarse binary* distance measurement. This also brings about the finite time formation convergence, as will be discussed in Section 4.

In the presence of quantized measurement and feedback, the right-hand side of (7) is discontinuous and we will consider the following differential inclusion

$$\dot{p}_i \in \mathcal{F}\left[\sum_{k=1}^{m} b_{ik}\, q(||z_k|| - d_k)\, \hat{z}_k\right]. \tag{8}$$

In the following, we define the distance error for edge k as $e_k = ||z_k|| - d_k$. We then calculate the differential inclusion $\mathcal{F}(q(e_k))$ which will be used in later analysis. In the case of a symmetric uniform quantizer, the differential inclusion $\mathcal{F}(q_u(e_k))$ can be calculated as

$$\mathcal{F}(q_u(e_k)) = \begin{cases} h\delta_u, & e_k \in \left((h-\frac{1}{2})\delta_u, (h+\frac{1}{2})\delta_u\right), h \in \mathbb{Z}; \\ [h\delta_u, (h+1)\delta_u], & e_k = (h+\frac{1}{2})\delta_u, h \in \mathbb{Z}. \end{cases}$$

Note that $e_k\mathcal{F}(q_u(e_k)) \geq 0$ for all e_k, and $e_k\mathcal{F}(q_u(e_k)) = 0$ if and only if $e_k \in [-\frac{\delta_u}{2}, \frac{\delta_u}{2}]$. We refer the reader to Section 2.3 for the definition and meaning of notations such as δ_u and h.

In the case of a logarithmic quantizer, the differential inclusion $\mathcal{F}(q_l(e_k))$ can be calculated as

$$\mathcal{F}(q_l(e_k)) = \begin{cases} \text{sign}(e_k)\text{exp}(q_u(\ln|e_k|)), & e_k \neq e^{(h+\frac{1}{2})\delta_u}, h \in \mathbb{Z}; \\ [\text{exp}(h\delta_u), \text{exp}((h+1)\delta_u)], & e_k = e^{(h+\frac{1}{2})\delta_u}, h \in \mathbb{Z}. \end{cases}$$

Also note that $e_k\mathcal{F}(q_l(e_k)) > 0$ for all $e_k \neq 0$, and $e_k\mathcal{F}(q_l(e_k)) = 0$ if and only if $e_k = 0$.

We define the distance error vector as $e = [e_1, e_2, \ldots, e_m]^\top$. Then in a compact form, one can rewrite the dynamics of (8) as

$$\dot{p} \in \mathcal{F}\Big[-\overline{B} D_{\hat{z}}\, q\Big(e(\underset{k}{\text{col}}\left(\|z_k\|\right)\Big)\Big]. \tag{9}$$

In order not to overload the notation, here by $\hat{z}$ we exclusively mean the vector-wise normalization of z, therefore $D_{\hat{z}}$ in the above equation and in the sequel is defined as $D_{\hat{z}} = \text{diag}\{\hat{z}_1, ..., \hat{z}_m\}$. This notation rule will also be applied to $\tilde{z}$ in the sequel. Note that the differential inclusion $\mathcal{F}(q(e))$ with the vector e is defined according to the product rule of Filippov's calculus properties (see [28]).

Example 1

We show an example to illustrate the formation control system with quantized measurements. Consider a formation system aiming to achieve a double tetrahedron shape in 3-D space (see Figure 2), which consists of five agents labeled by $1, 2, 3, 4, 5$ and nine edges. The formation is minimally rigid. For the purpose of writing an oriented incidence matrix, suppose that the nine edges are oriented from i to j just when $i < j$. Then we can number the edges in the following order: $12, 13, 14, 23, 34, 24, 25, 35, 45$. Thus, the following oriented incidence matrix for the undirected graph in Figure 2 can be obtained

$$B = \begin{bmatrix} -1 & -1 & -1 & 0 & 0 & 0 & 0 & 0 & 0 \\ 1 & 0 & 0 & -1 & 0 & -1 & -1 & 0 & 0 \\ 0 & 1 & 0 & 1 & -1 & 0 & 0 & -1 & 0 \\ 0 & 0 & 1 & 0 & 1 & 1 & 0 & 0 & -1 \\ 0 & 0 & 0 & 0 & 0 & 0 & 1 & 1 & 1 \end{bmatrix} \tag{10}$$

DOI: 10.1002/rnc

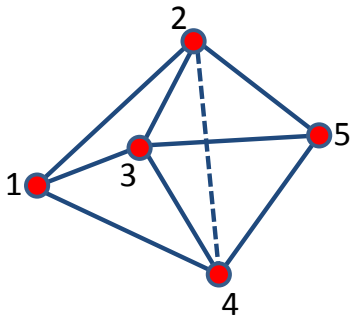

Figure 2. A 3-D double tetrahedron formation shape, with 5 agents and 9 distances.

The composite relative position vector z is then defined according to the orientation for each edge, as in the incidence matrix B, in the form of $z = \overline{B}^{\top} p$. As an example, one has $z_1 = p_2 - p_1$, i.e. the vector z_1 at edge 1 is defined by the relative position between agent 2 and agent 1. The formation dynamics for agent 1 can be written as

$$\dot{p}_1 \in \mathcal{F}\left[q(||z_1|| - d_1)\,\hat{z}_1 + q(||z_2|| - d_2)\hat{z}_2 + q(||z_3|| - d_3)\hat{z}_3\right]. \tag{11}$$

and similarly one can obtain the system equation for other agents.

By defining the matrix $\overline{B}$ and $D_{\hat{z}}$, one can obtain compact equations of system dynamics in the compact form of (9).

3.2. *Properties of quantized formation control systems*

We first discuss the solution issue of the formation control system (8). However, it is more convenient to focus on the dynamics of the relative position vector z, which can be derived from (8) as follows

$$\dot{z} = \overline{B}^{\top}\dot{p} \in \mathcal{F}\Big[-\overline{B}^{\top}\overline{B}D_{\hat{z}}\,q\Big(e(\operatorname*{col}_k\left(\|z_k\|\right)\Big)\Big]. \tag{12}$$

First note that at any non-collocated finite initial point $p(0)$, the right-hand side of (8) and of (12) is measurable and locally essentially bounded. Thus, the existence of a local Filippov solution of (8) and of (12) starting at such initial points is guaranteed.

We then derive a dynamical system from (9) to describe the evolution of the distance error vector e. According to the definition of the distance error e_k, e_k is a smooth function of z_k. Thus, by using the calculus property (see [25]) and the set-valued Lie derivative computation theorem (see [29]), one can show $\dot{e}_k$ exists and $\dot{e}_k = \frac{1}{\|z_k\|} z_k^{\top}\dot{z}_k$ holds almost everywhere. The dynamics for the distance error vector e can be obtained in a compact form as

$$\begin{aligned}\dot{e} &= D_{\tilde{z}}D_z^{\top}\dot{z} = D_{\tilde{z}}D_z^{\top}\overline{B}^{\top}\dot{p} = D_{\tilde{z}}R(z)\dot{p}, \quad \text{a. e.}\\ &\in -\mathcal{F}\left[D_{\tilde{z}}R(z)R^{\top}(z)D_{\tilde{z}}q(e)\right], \quad \text{a. e.}\end{aligned} \tag{13}$$

A more general compact form of the system equation $\dot{e}$ can be found in [19, Section III]. Again, the existence of a local Filippov solution of (13) starting with a non-collocated finite initial point $p(0)$ is guaranteed. In the next section, we will also show that the solutions to (13) (as well as the solutions to (8) and (12)) are *bounded* and can be extended to $t \to \infty$ when agents' initial positions are chosen non-collocated and close to a target formation shape. Also, as shown in [18], when the formation shape is close to the desired one, the entries of the matrix $R(z)R^{\top}(z)$ are continuously differentiable functions of e. Since the nonzero entries of the diagonal matrix $D_{\tilde{z}}$ are of the form $\frac{1}{\|z_k\|}$ which are also continuously differentiable functions of e, we conclude that the system described in (13) is a self-contained system, and we will call it *the distance error* system in the sequel.

DOI: 10.1002/rnc

***Example** 2*
(Continued) We again use the formation shape shown in Figure 2 to illustrate the derivation of the above system equations.

According to the definition of the relative position vector z one can derive the compact form of the system dynamic equation for z, as shown in (12). From the construction of the incidence matrix B and the relative position vector z, the rigidity matrix can be obtained as

$$R = \begin{bmatrix} -z_1^\top & z_1^\top & 0 & 0 & 0 \\ -z_2^\top & 0 & z_2^\top & 0 & 0 \\ -z_3^\top & 0 & 0 & z_3^\top & 0 \\ 0 & -z_4^\top & z_4^\top & 0 & 0 \\ 0 & 0 & -z_5^\top & z_5^\top & 0 \\ 0 & -z_6^\top & 0 & z_6^\top & 0 \\ 0 & -z_7^\top & 0 & 0 & z_7^\top \\ 0 & 0 & -z_8^\top & 0 & z_8^\top \\ 0 & 0 & 0 & -z_9^\top & z_9^\top \end{bmatrix} \tag{14}$$

From the expression of the matrix $R(z)$ in (14), it is obvious that the entries of the matrix product $R(z)R^\top(z)$ are either zero, or inner products of relative position vectors in the form of $z_i^\top z_j$, which are functions of the distance error vector e (for detailed analysis, see e.g., [14, 18]). Since the diagonal matrix $D_{\tilde{z}}$ is defined as $D_{\tilde{z}} = \mathrm{diag}\{\tilde{z}_1, ..., \tilde{z}_9\}$ with $\tilde{z}_k = \frac{1}{\|z_k\|}$, it is clear that the entries of the matrix $D_{\tilde{z}}$ are also functions of e, and therefore the entries in the matrix product $D_{\tilde{z}}R(z)R^\top(z)D_{\tilde{z}}$ are functions of e. Hence, the distance error system in (13) is a self-contained system, for which we can apply the Lyapunov argument to show its stability. Note the compact form of the error system (13) can be derived by the definition of the distance error e.

Finally, we show some additional properties of the formation control system with quantized information. Note that through this paper we assume that the underlying graph modelling inter-agent interactions is undirected.

***Lemma** 1*
In the presence of the uniform/logarithmic quantizer, the formation centroid remains stationary.

Proof
Denote by $p_c \in \mathbb{R}^d$ the center of the mass of the formation, i.e., $p_c = \frac{1}{n}\sum_{i=1}^n p_i = \frac{1}{n}(\mathbf{1}_n \otimes I_{d\times d})^\top p$. By applying the calculus property for the set-valued Lie derivative (see [25] or [29]), one has

$$\begin{aligned} \dot{p}_c(t) =& \frac{1}{n}(\mathbf{1}_n \otimes I_{d\times d})^\top \dot{p} \\ \in& -\frac{1}{n}(\mathbf{1}_n \otimes I_{d\times d})^\top R^\top(z) D_{\tilde{z}} \mathcal{F}[q(e(z))] \ \text{ for a.e. } t. \end{aligned} \tag{15}$$

Note that $(\mathbf{1}_n \otimes I_{d\times d})^\top R^\top(z) = \mathbf{0}$. Therefore,

$$\dot{p}_c(t) \in -\frac{1}{n}(\mathbf{1}_n \otimes I_{d\times d})^\top R^\top(z) D_{\tilde{z}} \mathcal{F}[q(e(z))] = \{0\} \text{ for a.e. } t. \tag{16}$$

Thus $\dot{p}_c = 0$ for a.e. t, which indicates that the position of the formation centroid remains constant. □

***Lemma** 2*
To implement the control, each agent can use its own local coordinate system to measure the relative position (quantized distance and unquantized bearing) of its neighbors, and a global coordinate system is not involved.

Note that the above lemma implies the $SE(N)$ invariance (i.e., translational and rotational invariance) [30] of the proposed formation controller, which enables a convenient implementation of the quantized formation control law without coordinate frame alignment for all of the agents. We refer the readers to [30] for a general treatment on coordinate frame issues in networked control systems.

DOI: 10.1002/rnc

Proof
The key part in the proof of local coordinate requirement is to show the control function for all the agents is an *SE(N)*-invariant function [†]. The control function for agent i is $f_i = \sum_{k=1}^{m} b_{ik}\, q(||z_k|| - d_k)\, \hat{z}_k$. Given an arbitrary coordination rotation $R \in SO(N)$ and displacement of origin $\omega \in \mathbb{R}^N$, there holds

$$\begin{aligned} f_i(Rp_1 + \omega, \ldots, Rp_n + \omega) &= \sum_{k=1}^{m} b_{ik}\, q(||z_k|| - d_k)\, R\, \hat{z}_k \\ &= R \sum_{k=1}^{m} b_{ik}\, q(||z_k|| - d_k)\, \hat{z}_k \\ &= R f_i(p_1, \ldots, p_n) \end{aligned} \tag{17}$$

and the statement is proved. □

3.3. Convergence analysis

In this section we aim to prove the following convergence result.

***Theorem** 1*
Suppose the target formation is infinitesimally and minimally rigid and the formation controller with quantized measurement is applied.

- In the case of a uniform quantizer, the formation converges locally to an approximately correct and static shape defined by the set $F_{\text{approx}} = \{e | e_k \in [-\frac{\delta_u}{2}, \frac{\delta_u}{2}], k \in \{1, \ldots, m\}\}$;
- In the case of a logarithmic quantizer, the formation converges locally to a correct and static formation shape.

In the proof we will use the Lyapunov theory of nonsmooth analysis, for which we construct a Lyapunov function candidate as

$$V(e) = \sum_{k=1}^{m} V_k(e_k), \text{ with } V_k(e_k) = \int_0^{e_k} q(s)\mathrm{d}s. \tag{18}$$

Before giving the proof of Theorem 1, we first show some properties of the function V defined in (18). For the definition of *function regularity* in nonsmooth analysis, see e.g. [31, Chapter 2] or [25, Page 57].

***Lemma** 3*
The function V constructed in (18) is positive semidefinite, and is regular everywhere.

Proof
The positive semidefiniteness of V is obvious from the property of the quantization functions q_u and q_l. Note that $V(e) = 0$ if and only if $e \in \{e | e_k \in [-\frac{\delta_u}{2}, \frac{\delta_u}{2}], k \in \{1, \ldots, m\}\}$ for a uniform quantizer q_u, or when $e = 0$ for a logarithmic quantizer q_l. The proof for the regularity is omitted here but follows similarly to the proof of the previous paper [6, Lemma 6]. We note a key fact that supports the regularity statement of V: V is continuously differentiable almost everywhere, while at the nondifferentiable points V has corners of *convex* type. From the sufficient condition of regular functions stated in [32, Page 200], [‡] this key fact implies that V is regular everywhere. □

[†] A function f is said to be *SE(N)*-invariant if for all $R \in SO(N)$ and all $x_1, \ldots, x_n, \omega \in \mathbb{R}^N$, there holds $Rf(x_1, \ldots, x_n) = f(Rx_1 + \omega, \ldots, Rx_n + \omega)$.
[‡] "Roughly speaking, we can think of regular functions as those that, at each point, are either smooth, or else have a corner of convex type" [32, Page 200].

DOI: 10.1002/rnc

Furthermore, according to the definition of generalized derivative (see e.g. [31, Chapter 2]), one can calculate the generalized derivative of V_k (for the case of a uniform quantizer) as

$$\partial V_k = \begin{cases} [h\delta_u, (h+1)\delta_u], & e_k = (h+\frac{1}{2})\delta_u, h \in \mathbb{Z} \\ q(e_k), & \text{elsewise} \end{cases}$$

Similarly, one can also calculate the generalized derivative of $V_k(e_k)$ for the case of a logarithmic quantizer (which is omitted here). The generalized derivative of $V(e)$ can be obtained by the product rule (see [25, Page 50]). Now we are ready to prove Theorem 1.

Proof

We choose the Lyapunov function constructed in (18) for the distance error system (13) with discontinuous right-hand side. Note that $R(z)R^\top(z)$ and $D_{\tilde{z}}$ are positive definite matrices at the desired formation shape. Similarly to the analysis in [14] and in [19], we define a sub-level set $\mathcal{B}(\rho) = \{e : V(e) \leq \rho\}$ for some suitably small ρ, such that when $e \in \mathcal{B}(\rho)$ the formation is infinitesimally minimally rigid and the initial formation shape is close enough to the prescribed shape (which implies that inter-agent collisions cannot be possible). Note that all these imply that $R(z)R^\top(z)$ and $D_{\tilde{z}}$ are *positive definite* when $e \in \mathcal{B}(\rho)$. Note also that the defined sub-level set $\mathcal{B}(\rho)$ is compact, and the matrix $Q(e) := D_{\tilde{z}}R(z)R^\top(z)D_{\tilde{z}}$ is also *positive definite* when $e \in \mathcal{B}(\rho)$. As a consequence, in the following we rewrite the distance error system as $\dot{e} \in \mathcal{F}[-Q(e)q(e)]$.

The regularity of V shown in Lemma 3 allows us to employ the nonsmooth Lyapunov theorem [29, Section 2] to develop the stability analysis. We calculate the set-valued derivative of V along the trajectory of the distance error system (13). By applying the calculation rule for the set-valued derivative (see [25, Pages 62-63]), one can obtain

$$\begin{aligned} \dot{V}(e)_{(13)} \in \tilde{\mathcal{L}}_{(13)}V(e) = \{a \in \mathbb{R} | \exists v \in \dot{e}_{(13)}, \\ \text{such that } \zeta^\top v = a, \forall \zeta \in \partial V(e)\}. \end{aligned} \tag{19}$$

Note that the set $\tilde{\mathcal{L}}_{(13)}V(e)$ could be empty, and in this case we adopt the convention that $\max(\emptyset) = -\infty$. When it is not empty, there exists $v \in -Q(e)q(e)$ such that $\zeta^\top v = a$ for all $\zeta \in \partial V(e)$. A natural choice of v is to set $v \in -Q(e)\zeta$, with which one can obtain $a = -q^\top(e)Q(e)q(e)$. Let $\bar{\lambda}_{\min}$ denote the smallest eigenvalue of $Q(e)$ when $e(p)$ is in the compact set $\mathcal{B}$ (i.e. $\bar{\lambda}_{\min} = \min_{e\in\mathcal{B}} \lambda(Q(e)) > 0$). Note that $\bar{\lambda}_{\min}$ exists because the set $\mathcal{B}$ is a compact set and the eigenvalues of a matrix are continuous functions of the matrix elements, and $\bar{\lambda}_{\min} > 0$ because $Q(e)$ is *positive definite* with $e \in \mathcal{B}(\rho)$ as mentioned above. Then if the set $\tilde{\mathcal{L}}_{(13)}V(e)$ is not empty, one can show

$$\max(\tilde{\mathcal{L}}_{(13)}V(e)) \leq -\bar{\lambda}_{\min}q(e)^\top q(e) \tag{20}$$

and if the set $\tilde{\mathcal{L}}_{(13)}V(e)$ is empty, one has $\max(\tilde{\mathcal{L}}_{(13)}V(e)) = -\infty$. Note that both cases imply that V is non-increasing, and consequently the Filippov solution $e(t)$ of (13) is bounded. Thus, all solutions to (13) (as well as the solutions to (8)) are bounded and can be extended to $t = \infty$ (i.e., there is no finite escape time).

We now divide the rest of the proof into two parts, according to different quantizers:

- The case of uniform quantizers: it can be seen that $\max(\tilde{\mathcal{L}}_{(13)}V(e)) \leq 0$ for all $e \in \mathcal{B}(\rho)$ and $0 \in \max(\tilde{\mathcal{L}}_{(13)}V(e))$ if and only if $e \in F_{\text{approx}}$. Also note that F_{approx} is compact, and is positively invariant for the distance error system (13) (i.e. if the initial formation is such that $e(0) \in F_{\text{approx}}$, then all agents are static and $e(t) \in F_{\text{approx}}$ for all t). According to the nonsmooth invariance principle [29, Theorem 3], the first part of the convergence result is proved. Since this is a convergence to a *closed and bounded* set F_{approx} (i.e., a compact set), and outside this set the set-valued derivative of V along the trajectory of the distance error system is always negative (i.e., $\max(\tilde{\mathcal{L}}_{(13)}V(e)) < 0$ for $e \in \mathcal{B}(\rho) \setminus F_{\text{approx}}$) while $\mathcal{B}(\rho)$ is also a compact set, the convergence to F_{approx} is achieved within a *finite time*. Note also from (7) the final formation is stationary because $\dot{p}(t) = 0$ for $e(t) \in F_{\text{approx}}$.

DOI: 10.1002/rnc

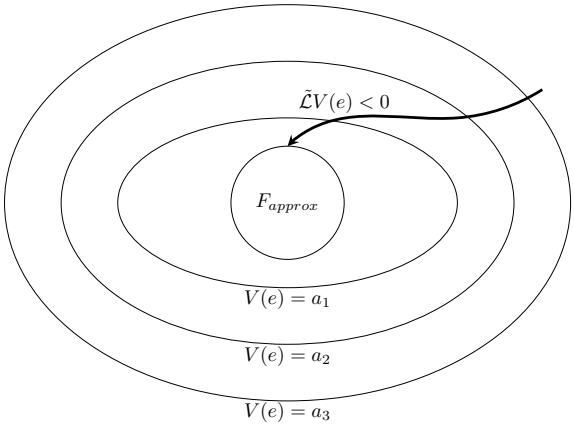

Figure 3. Illustration of finite time convergence to a compact set $F_{\text{approx}(e)}$ centered at $e = 0$. Outside this set F_{approx} the set-valued derivative of V along the trajectory of the distance error system is always negative. In the figure, three level sets of $V(e)$ with $a_3 > a_2 > a_1$ are shown, which are compact sets with respect to e. Note as also shown in the figure $V(e)$ is a positive definite and strictly increasing function of e.

- The case of logarithmic quantizers: it can be seen that $\max(\tilde{\mathcal{L}}_{(13)}V(e)) \leq 0$ for all $e \in \mathcal{B}(\rho)$ and $0 \in \max(\tilde{\mathcal{L}}_{(13)}V(e))$ if and only if $e = 0$. According to the nonsmooth invariance principle [29, Theorem 3], the second part of the convergence result is proved. Also note from (7) the final formation is stationary.

The proof is thus completed. □

Remark 2
(**Finite time convergence to a compact set**) In the above we have shown the trajectories of distance errors in the formation system under uniform quantization converge to a bounded and closed set F_{approx} within a finite time, the size of which also depends on the uniform quantizer errors. The key recipes to guarantee the finite time convergence are the following: (i) the set F_{approx} and the sublevel sets $V(e)$ are compact sets; (ii) Outside the set F_{approx} the set-valued derivative of V along the trajectories of the distance error system is always negative; and (iii) the function $V(e)$ is a strictly increasing function of e. An intuitive illustration of the finite time convergence of distance error trajectories to the set F_{approx} is shown in Figure 3.

Remark 3
We now show a stronger convergence result (i.e., convergence to a point in the set) in addition to the finite time convergence in the case of uniform quantizers (2). We observe that a sufficient condition for the position p_i of agent i to converge to a fixed point is that $\int_0^\infty \dot{p}_i(t)\mathrm{d}t < \infty$, which is true since (i) initially all agents are at finite positions (i.e., $p_i(0) < \infty$), and (ii) all $\dot{p}_i(t)$ (associated with the control input) are upper bounded and converge to the origin in *finite time*. By the integration law this implies $p_i(t)_{t>T}$ is constant at a fixed position when $e(t)_{t>T} \in F_{\text{approx}}$ where T is the finite settling time of convergence, which further implies that the distance error $e(t)$ converges to a fixed point in the set F_{approx}.

4. A SPECIAL QUANTIZER: FORMATION CONTROL WITH BINARY DISTANCE INFORMATION

4.1. Rigid formation control with coarse measurements

In this section we consider the special case in which each agent uses very coarse distance measurements, in the sense that it only needs to detect whether the current distance to each of its neighbors is greater or smaller than the desired distance. This gives rise to a special quantizer

DOI: 10.1002/rnc

defined by the following *signum* function:

$$\text{sign}(x) = \begin{cases} 1 & \text{when } x > 0; \\ 0 & \text{when } x = 0; \\ -1 & \text{when } x < 0. \end{cases}$$

Accordingly, we obtain the following rigid formation control system with *binary distance measurements*:

$$\dot{p}_i = -\sum_{k=1}^{m} b_{ik} \text{sign}(||z_k|| - d_k)\, \hat{z}_k \tag{21}$$

Remark 4
Formation control using the signum function has been discussed in several previous papers. In [33], a finite-time convergence was established for stabilization of cyclic formations using binary bearing-only measurements. A linear-consensus-based formation control with coarsely quantized measurements was discussed in [15], while the implementation of the controller requires a common sense of global coordinate frame orientation. The work closest to the controller setting in this section is the paper [17], which studied the stabilization control of a cyclic triangular formation with the controller (21). Here we extend such controllers to stabilize a general undirected formation which is minimally and infinitesimally rigid. The above controller (21) can also be seen as a high-dimensional extension of the one-dimensional formation controller studied in [34].

Remark 5
Note that the right-hand side of (21) is composed of the sum of a unit vector multiplied by a signum function. This implies that the formation controller (21) is of special interest in practice since the control action is explicitly upper bounded by the cardinality of the set of neighbors for each agent i, which prevents potential implementation problems due to saturation.

Again, we consider the Filippov solution to the formation control system (21). The differential inclusion $\mathcal{F}(\text{sign}(e_k))$ can be calculated as

$$\mathcal{F}(\text{sign}(e_k)) = \begin{cases} 1 & \|z_k\| > d_k, \\ [-1, 1], & \|z_k\| = d_k, \\ -1 & \|z_k\| < d_k. \end{cases}$$

In a compact form, the rigid formation system (21) can be rewritten as

$$\dot{p} \in \mathcal{F}[-R^{\top}(z) D_{\tilde{z}} \text{sign}(e)], \tag{22}$$

where $\text{sign}(e)$ is defined in a component-wise way.

Note that the right-hand side of (22) is measurable and essentially bounded at any non-collocated and finite point p, and the existence of a local Filippov solution to (22) is guaranteed from such an initial point $p(0)$. In the following analysis we will also show that the solutions are bounded and complete.

Similar to the analysis in deriving the distance error system shown in Section 3.2, the distance error system with binary distance information can be obtained as

$$\dot{e} \in \mathcal{F}[-D_{\tilde{z}} R(z) R^{\top}(z) D_{\tilde{z}} \text{sign}(e)], \quad \text{a. e.} \tag{23}$$

Again, similar to the analysis for (13), one can also show that (23) is a self-contained system when e takes values locally around the origin.

4.2. *Convergence analysis*

The main result in this section is stated in the following convergence theorem for the formation controller (22) with binary distance information.

DOI: 10.1002/rnc

***Theorem** 2*
Suppose the target formation is infinitesimally and minimally rigid, the initial formation shape is close to the target formation shape, and the formation controller (21) with binary distance information is applied.

- The formation converges locally to a static target formation shape;
- The convergence is achieved within a finite time upper bounded by $T^* = \frac{\|e(0)\|_1}{\bar{\lambda}_{\min}}$ where $\bar{\lambda}_{\min}$ is defined in the proof.

Proof
Part of the proof for this theorem is similar to the proof of Theorem 1. Choose the Lyapunov function defined as $V = \sum_{k=1}^{m} V_k(e_k)$ with $V_k(e_k) = |e_k|$ for the distance error system (23). Note that V is a convex and regular function of e. Also V is locally Lipschitz at $e = 0$ and is continuously differentiable at all other points. The generalized derivative of $V_k(e_k)$ can be calculated as

$$\partial V_k = \begin{cases} 1, & e_k > 0; \\ [-1, 1], & e_k = 0; \\ -1, & e_k < 0. \end{cases}$$

and the generalized derivative of V can be calculated similarly via the product rule (see [25]). We define a sub-level set $\mathcal{B}(\rho) = \{e : V(e) \leq \rho\}$ for some suitably small ρ, such that when $e \in \mathcal{B}(\rho)$ the formation is infinitesimally minimally rigid and $R(z)R^\top(z)$ and $D_{\tilde{z}}$ are *positive definite*. Now the matrix $Q(e) := D_{\tilde{z}}R(z)R^\top(z)D_{\tilde{z}}$ is also *positive definite* when $e \in \mathcal{B}(\rho)$. Let $\bar{\lambda}_{\min}$ denote the smallest eigenvalue of $Q(e)$ when $e(p)$ is in the compact set $\mathcal{B}$ (i.e. $\bar{\lambda}_{\min} = \min_{e \in \mathcal{B}} \lambda(Q(e)) > 0$).

In the following, we calculate the set-valued derivative of V along the trajectory described by the differential inclusion (23). The argument follows similarly to the analysis in the proof of Theorem 1. By applying the calculation rule for the set-valued derivative (see [25, Pages 62-63]), one can obtain

$$\begin{aligned} \dot{V}(e)_{(23)} \in \tilde{\mathcal{L}}_{(23)}V(e) = \{a \in \mathbb{R} | \exists v \in \dot{e}_{(23)}, \\ \text{such that } \zeta^\top v = a, \forall \zeta \in \partial V(e)\}. \end{aligned} \tag{24}$$

If the set $\tilde{\mathcal{L}}_{(23)}V(e)$ is not empty, there exists $v \in -Q(e)\text{sign}(e)$ such that $\zeta^\top v = a$ for all $\zeta \in \partial V(e)$. A natural choice of v is to set $v \in -Q(e)\zeta$, with which one can obtain $a = -\text{sign}^\top(e)Q(e)\text{sign}(e)$. Then one can further show

$$\max(\tilde{\mathcal{L}}_{(23)}V(e)) \leq -\bar{\lambda}_{\min}\text{sign}(e)^\top\text{sign}(e), \tag{25}$$

if the set is not empty, while if it is empty we adopt the convention $\max(\tilde{\mathcal{L}}_{(23)}V(e)) = -\infty$. Note that this implies that V is non-increasing, and consequently the Filippov solution $e(t)$ is bounded. Thus, all solutions to (23) (as well as the solutions to (22)) are complete and can be extended to $t = \infty$ (i.e., there is no finite escape time). It can be seen that $\max(\tilde{\mathcal{L}}_{(23)}V(e)) \leq 0$ for all $e \in \mathcal{B}(\rho)$ and $0 \in \max(\tilde{\mathcal{L}}_{(23)}V(e))$ if and only if $e = 0$. According to the nonsmooth invariance principle [29, Theorem 3], the asymptotic convergence is proved.

We then prove the stronger convergence result, i.e., the finite-time convergence. From the definition of the *sign* function in (21), there holds $\text{sign}(e)^\top\text{sign}(e) > 1$ for any $e \neq 0$, which implies

$$\max(\tilde{\mathcal{L}}_{(23)}V(e)) \leq -\bar{\lambda}_{\min} \tag{26}$$

for any $e \neq 0$. Thus, by applying the Finite-time Lyapunov Theorem [35], any solution starting at $e(0) \in \mathcal{B}(\rho)$ reaches the origin in finite time, and the convergence time is upper bounded by $T^* = V(e(0))/\bar{\lambda}_{\min} = \|e(0)\|_1/\bar{\lambda}_{\min}$. □

Remark 6
(**Finite time formation convergence**) Different to the finite time convergence to an approximate

Prepared using rncauth.cls
DOI: 10.1002/rnc

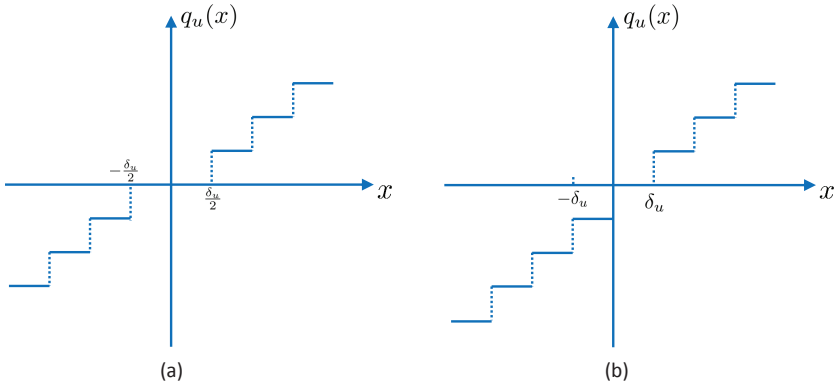

Figure 4. (a) Symmetric uniform quantizer function, defined in (2). (b) Asymmetric uniform quantizer function, defined in (27).

formation shape under uniform quantizers as shown in Theorem 1, in Theorem 2 it is shown the formation system converges locally to a correct formation shape under binary distance measurements, which is a more desirable convergence result. Also, compared to the finite time formation controller discussed in the paper [36] in which a sig function is used, the finite time formation controller in (21) requires less information in the distance measurements, in which very coarse measurements in terms of binary signals are sufficient.

Remark 7
(**Dealing with chattering**) In the controller (21) the sign function is used, which may cause chattering of the solutions to the formation system when the formation is very close to the desired one (i.e. when e is very close to the origin). This is because in practice imperfections (e.g., perturbations in measurements or delays) could cause agents' state trajectories to 'chatter' across the discontinuity surface (see e.g. [37, Chapter 3.5]). Possible solutions to eliminate the chattering include the following:

- Add deadzone (approximated by smooth functions) to the sign function around the origin (similar to the case of uniform quantizers; see Part 1 of Theorem 1). This will give rise to a trade-off in the convergence, i.e., the distance error does not converge to the origin but to a bounded set, the size of which depends on (for a fixed number of agents) how large the deadzone parameter is chosen (see e.g. [38, 39]);
- Use the hysteresis principle in the quantization function design [5].

The adoption of the above techniques to avoid chattering will be discussed in future research.

5. ASYMMETRIC UNIFORM QUANTIZER

In [6], it has been shown that when an *asymmetric* uniform quantizer (defined below) is applied to double-integrator consensus dynamics some undesirable motions may occur. In this section we investigate whether there are undesired motions for rigid formation control in the presence of an asymmetric uniform quantizer.

We consider the following *asymmetric* uniform quantizer (the same as in [6]), defined by

$$q_u^*(x) = \delta_u \left(\left\lfloor \frac{x}{\delta_u} \right\rfloor \right), \tag{27}$$

where δ_u is a positive number and $\lfloor a \rfloor, a \in \mathbb{R}$ denotes *the greatest integer that is less than or equal to* a. For a comparison of the uniform quantizers defined in (2) and in (27), see Fig. 4.

DOI: 10.1002/rnc

5.1. Motivating example: two-agent formation case

We first consider a two-agent formation case. Suppose two agents are controlled to achieve an inter-agent distance of d_{12} with the quantization function (27). The system dynamics for agents 1 and 2 can be described, respectively, as

$$\dot{p}_1 = q_u^* \left(||z_1|| - d_{12} \right) \hat{z}_1 \tag{28}$$

and

$$\dot{p}_2 = -q_u^* \left(||z_1|| - d_{12} \right) \hat{z}_1 \tag{29}$$

where $z_1 = p_2 - p_1$, and $q_u^*(\cdot)$ denotes the asymmetric uniform quantizer in (27).

***Lemma** 4*
Consider the two-agent formation control system (28) and (29) with the asymmetric quantization function (27).

- If the initial distance between agents 1 and 2 is greater than $d_{12} + \delta_u$, then the inter-agent distance $\|z\|$ will converge to $d_{12} + \delta_u$ and the final formation will be stationary;
- If the initial distance between agents 1 and 2 is smaller than the desired distance d_{12}, then the inter-agent distance $\|z\|$ will converge to the desired distance d_{12} and the final formation will be stationary;
- If the initial distance between agents 1 and 2 is between d_{12} and $d_{12} + \delta_u$, then both agents 1 and 2 remain stationary and the inter-agent distance $\|z\|$ remains unchanged.

The proof is obvious and is omitted here as it can be inferred from previous proofs.

Remark 8
In the above example it can be seen that in the case of an asymmetric uniform quantizer, there exist no undesired motions, which is different to the result observed in [6] which showed unbounded velocities. Apart from the difference in system dynamics under discussions, the key difference that leads to the distinct behaviors is that when the asymmetric quantizer is applied to the consensus dynamics (which is to quantize a vector), there holds $\mathcal{F}[q_u^*(r_i - r_j)] + \mathcal{F}[q_u^*(r_j - r_i)] = -\delta_u$ when $r_j - r_i \neq k\delta_u$, where $r_j - r_i$ denotes the relative position vector (see Section 5 of [6]). Note that in the above formation controller, the quantization applies only to the distance error term (i.e. $q_u^* \left(\|p_2 - p_1\| - d_{12} \right)$) which is a scalar, and the asymmetric property of the quantizer only affects the convergence of the distance term.

5.2. General formation case

We consider the general formation case with more than two agents, in which each agent employs asymmetric uniform quantizers in individual controllers.

***Theorem** 3*
Suppose each individual agent takes the asymmetric uniform quantizer (27) in the quantized formation controller (7). Then the inter-agent distances converge within a finite time to the set

$$F_{\text{aym}} = \{e | e_k \in [0, \delta_u], k \in \{1, \ldots, m\}\}.$$

The proof is omitted here as it can be directly inferred from the previous proof of Theorem 1.

6. ILLUSTRATIVE EXAMPLES AND SIMULATIONS

In this section we show several numerical examples to illustrate the theoretical results obtained in previous sections. In the following illustrative examples we consider the stabilization control of a five-agent minimally rigid formation in the 3-D space, as a continuation of Example 1.

DOI: 10.1002/rnc

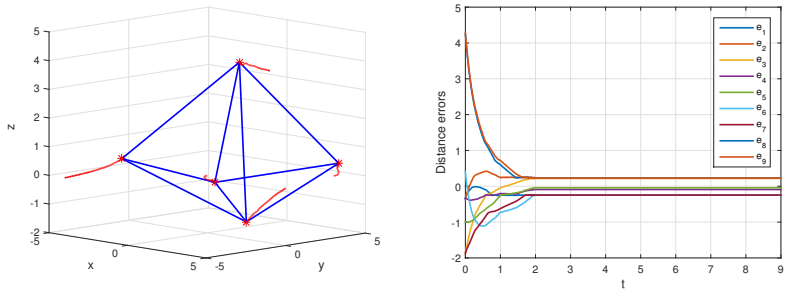

Figure 5. Stabilization control of a rigid formation: symmetric uniform quantization case. Left: the trajectories of five agents and the final formation shape. Right: Time evolutions of the distance errors. It is obvious from the right figure that the formation shape converges to an approximately correct one in a finite time.

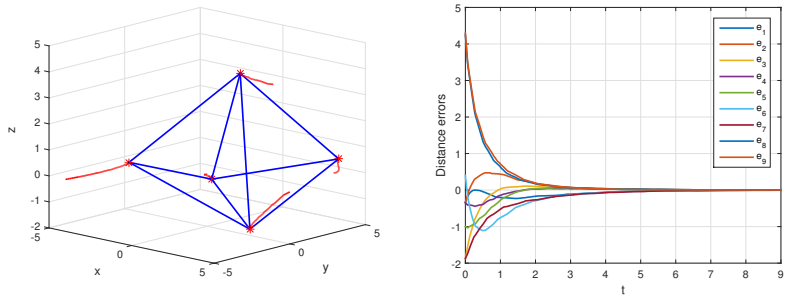

Figure 6. Stabilization control of a rigid formation: logarithmic quantization case. Left: the trajectories of five agents and the final formation shape. Right: Time evolutions of the distance errors.

The underlying graph describes a double tetrahedron shape of nine edges (see Figure 2 for an illustration), and the desired distances for all edges are set as 6. [§] The initial positions are chosen such that the initial formation is infinitesimally rigid and is close to a target formation shape. For all simulations, we set the quantization gain as $\delta_u = 0.5$.

Agents trajectories, the final formation shape and the evolutions of nine distance errors under symmetric uniform quantization and under logarithmic quantization are shown in Figure 5 and Figure 6, respectively. It is obvious from these two figures that with symmetric uniform quantizer the formation errors converge to the bounded set $F_{\text{approx}} = \{e | e_k \in [-0.25, 0.25], k \in \{1, \ldots, m\}\}$ in a *finite time*, and with the logarithmic quantizer the formation converges to the target shape asymptotically, which are consistent with the theoretical results in Theorem 1.

The formation convergence behavior with binary distance measurements under the quantization strategy (21) is depicted in Figure 7. It can be seen from Figure 7 that with very coarsely quantized distance measurement via a simple signum function as in (21), the formation converges to the target shape within a finite time, but the price to be paid is the occurrence of chattering (as shown in the right part of Figure 7).

Finally, when the asymmetric uniform quantizer (27) is used in the formation control system (7), the formation converges to an approximate one with all distance errors converging to the bounded set $F_{\text{aym}} = \{e | e_k \in [0, 0.5], k \in \{1, \ldots, m\}\}$ within a finite time, as shown in Figure 8. This supports the conclusion of Theorem 3.

[§]Note that the realization of a target formation with the given nine desired distances is not unique up to rotation and translation [23].

DOI: 10.1002/rnc

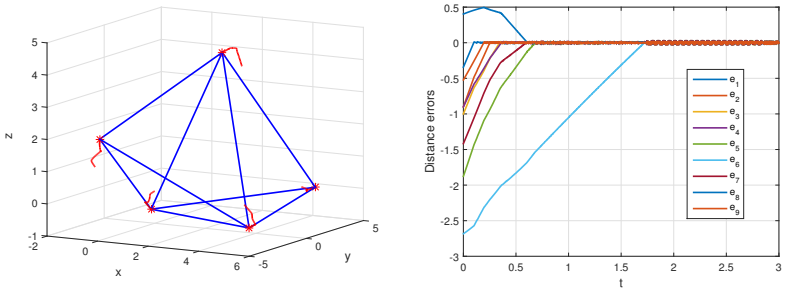

Figure 7. Stabilization control of a rigid formation: binary measurement case. Left: the trajectories of five agents and the final formation shape. Right: Time evolutions of the distance errors.

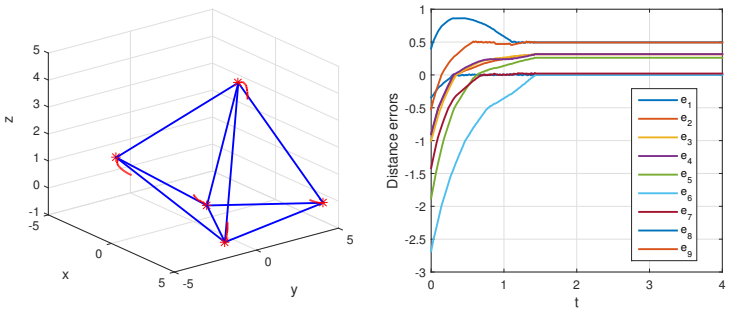

Figure 8. Stabilization control of a rigid formation: asymmetric uniform quantization case. Left: the trajectories of five agents and the final formation shape. Right: Time evolutions of the distance errors.

7. CONCLUDING REMARKS

In this paper we consider the rigid formation control problem with quantized distance measurements. We have discussed in detail the quantization effect on the convergence of rigid formation shapes under two commonly-used quantizers. In the case of the symmetric uniform quantizer, all distances will converge locally to a bounded set, the size of which depends on the quantization error. In the case of the logarithmic quantizer, all distances converge locally to the desired values. We also consider a special quantizer with a signum function, which allows each agent to use very coarse distance measurements (i.e. binary information on whether it is close or far away to neighboring agents with respect to the desired distances). We show in this case the formation shape can still be achieved within a finite time. We further discuss the case of an asymmetric quantizer applied in rigid formation control system, and analyze the convergence property of distance errors.

ACKNOWLEDGMENT

This work was supported by the Australian Research Council under grant DP130103610 and DP160104500. Z. Sun was supported by the Prime Minister's Australia Asia Incoming Endeavour Postgraduate Award.

REFERENCES

1. Brockett RW, Liberzon D. Quantized feedback stabilization of linear systems. *IEEE Transactions on Automatic Control* 2000; **45**(7):1279–1289.
2. Liberzon D. Hybrid feedback stabilization of systems with quantized signals. *Automatica* 2003; **39**(9):1543–1554.

3. Kashyap A, Başar T, Srikant R. Quantized consensus. *Automatica* 2007; **43**(7):1192–1203.
4. Cai K, Ishii H. Quantized consensus and averaging on gossip digraphs. *IEEE Transactions on Automatic Control* 2011; **56**(9):2087–2100.
5. Ceragioli F, De Persis C, Frasca P. Discontinuities and hysteresis in quantized average consensus. *Automatica* 2011; **47**(9):1916–1928.
6. Liu H, Cao M, De Persis C. Quantization effects on synchronized motion of teams of mobile agents with second-order dynamics. *Systems & Control Letters* 2012; **61**(12):1157–1167.
7. Frasca P. Continuous-time quantized consensus: convergence of Krasovskii solutions. *Systems & Control Letters* 2012; **61**(2):273–278.
8. Guo M, Dimarogonas DV. Consensus with quantized relative state measurements. *Automatica* 2013; **49**(8):2531–2537.
9. Krick L, Broucke ME, Francis BA. Stabilisation of infinitesimally rigid formations of multi-robot networks. *International Journal of Control* 2009; **82**(3):423–439.
10. Dörfler F, Francis B. Geometric analysis of the formation problem for autonomous robots. *IEEE Transactions on Automatic Control* 2010; **55**(10):2379–2384.
11. Oh KK, Ahn HS. Distance-based undirected formations of single-integrator and double-integrator modeled agents in n-dimensional space. *International Journal of Robust and Nonlinear Control* 2014; **24**(12):1809–1820.
12. Oh KK, Park MC, Ahn HS. A survey of multi-agent formation control. *Automatica* 2015; **53**:424–440.
13. Sun Z, Helmke U, Anderson BDO. Rigid formation shape control in general dimensions: an invariance principle and open problems. *Proc. of the 54th Conference on Decision and Control*, IEEE, 2015; 6095–6100.
14. Sun Z, Mou S, Anderson BDO, Cao M. Exponential stability for formation control systems with generalized controllers: a unified approach. *Systems & Control Letters* 2016; **93**:50–57.
15. Jafarian M, Persis CD. Formation control using binary information. *Automatica* 2015; **53**:125 – 135.
16. Meng Z, Anderson BDO, Hirche S. Formation control with mismatched compasses. *Automatica* 2016; **69**:232–241.
17. Liu H, Garcia de Marina H, Cao M. Controlling triangular formations of autonomous agents in finite time using coarse measurements. *Proc. of IEEE International Conference on Robotics and Automation (ICRA)*, IEEE, 2014; 3601–3606.
18. Mou S, Belabbas M, Morse A, Sun Z, Anderson BDO. Undirected rigid formations are problematic. *IEEE Transactions on Automatic Control* 2016; **61**(10):2821–2836.
19. Garcia de Marina H, Jayawardhana B, Cao M. Distributed rotational and translational maneuvering of rigid formations and their applications. *IEEE Transactions on Robotics* 2016; **32**(3):684–697.
20. Park MC, Sun Z, Anderson BDO, Ahn HS. Stability analysis on four agent tetrahedral formations. *Proc. of the 2014 IEEE 53rd Annual Conference on Decision and Control (CDC)*, IEEE, 2014; 631–636.
21. Chen X, Belabbas MA, Başar T. Global stabilization of triangulated formations. *SIAM Journal on Control and Optimization* 2017; **55**(1):172–199.
22. Sun Z, Garcia de Marina H, Anderson BDO, Cao M. Quantization effects in rigid formation control. *Proc. of the 6th Australian Control Conference*, IEEE, 2016; 168–173.
23. Hendrickson B. Conditions for unique graph realizations. *SIAM journal on computing* 1992; **21**(1):65–84.
24. Anderson BDO, Yu C, Fidan B, Hendrickx JM. Rigid graph control architectures for autonomous formations. *IEEE Control Systems Magazine* 2008; **28**(6):48–63.
25. Cortés J. Discontinuous dynamical systems. *IEEE Control Systems Magazine* 2008; **28**(3):36–73.
26. Filippov AF. *Differential equations with discontinuous righthand sides*. Springer Science & Business Media, 1988.
27. Anderson BDO, Yu C, Dasgupta S, Morse AS. Control of a three-coleader formation in the plane. *Systems & Control Letters* 2007; **56**(9):573–578.
28. Paden B, Sastry S. A calculus for computing Filippov's differential inclusion with application to the variable structure control of robot manipulators. *IEEE Transactions on Circuits and Systems* 1987; **34**(1):73–82.
29. Bacciotti A, Ceragioli F. Stability and stabilization of discontinuous systems and nonsmooth lyapunov functions. *ESAIM: Control, Optimisation and Calculus of Variations* 1999; **4**:361–376.
30. Vasile C, Schwager M, Belta C. Translational and rotational invariance in networked dynamical systems. *IEEE Transactions on Control of Network Systems, DOI: 10.1109/TCNS.2017.2648499* 2017; :in press.
31. Clarke FH. *Nonsmooth analysis and control theory*. Springer Science & Business Media, 1998.
32. Clarke FH. *Functional analysis, calculus of variations and optimal control*. Springer Science & Business Media, 2013.
33. Zhao S, Lin F, Peng K, Chen BM, Lee TH. Finite-time stabilisation of cyclic formations using bearing-only measurements. *International Journal of Control* 2014; **87**(4):715–727.
34. De Persis C, Liu H, Cao M. Control of one-dimensional guided formations using coarsely quantized information. *Proc. of the 49th Conference on Decision and Control*, IEEE, 2010; 2257–2262.
35. Cortés J. Finite-time convergent gradient flows with applications to network consensus. *Automatica* 2006; **42**(11):1993–2000.
36. Sun Z, Mou S, Deghat M, Anderson BDO. Finite time distributed distance-constrained shape stabilization and flocking control for d-dimensional undirected rigid formations. *International Journal of Robust and Nonlinear Control* 2016; **26**(13):2824–2844.
37. Sastry SS. *Nonlinear systems: analysis, stability, and control*, vol. 10. Springer Science & Business Media, 2013.
38. Lee H, Utkin VI. Chattering suppression methods in sliding mode control systems. *Annual Reviews in control* 2007; **31**(2):179–188.
39. Gupta R, Ghosh A. Frequency-domain characterization of sliding mode control of an inverter used in dstatcom application. *IEEE Transactions on Circuits and Systems I: Regular Papers* 2006; **53**(3):662–676.